

8. IN VIVO STUDIES

8.1 Introduction

Animal simulation breakthroughs in drug delivery are on the brink of understanding and treating several cancers and offer considerable power to potentiate the insightful function of in vivo research (1).

Though the in vitro cell line screening techniques provide faster results in a cost-effective manner, only cytotoxic compounds are screened by these methods. Apart from cytotoxicity, the pharmacokinetics and toxicity evaluations are also important with a view to measure complete effectiveness of a compound. Cell line studies are inadequate to estimate the off-target effects which may contribute to the potency or toxicity of the novel formulation (2). Hence, the drug candidate/formulation progresses to in vivo animal testing after completion of the initial in vitro cell line studies. Animal studies are critical for understanding the fundamental processes that support in vivo tumor development as tumor cells grown in vitro are not necessarily analogous to those that develop in a human subject (3).

Among various models of cancer research, murine models are well known and commonly used models for research. Rats have been used as the traditional animal for basic and preclinical studies of cancer because it has number of advantages such as:

- ✓ The similarity of rats and human genomes.
- ✓ The low cost of housing and maintenance.
- ✓ The short gestation period and rapid reproduction rate and
- ✓ The rapid growth of implanted tumors.

Variety of preclinical murine models of cancer have been developed (eg. xenografts, genetically engineered, and syngeneic mice) to study the development and progression of cancer as well as to increase the understanding of the etiology and dissemination of cancer to overcome barriers to early detection and resistance to standard chemotherapy(4). Among commonly adopted cancer models, chemically induced primary malignancies in mammals have several advantages including the easy procedures, fruitful tumor generation and high analogy to clinical human primary cancers.

Chemical carcinogens can be classified upon their origins such as environmental pollutants, cooked meat derived carcinogens, N-nitroso compounds, food additives, antineoplastic agents, naturally occurring substances and synthetic carcinogens, etc (5). Carcinogen-induced models

of primary cancers can be used to evaluate the diagnostic/therapeutic effects of drugs, investigate the biological factors, and explore preventive measures for carcinogenicity. The chemically induced cancer model is generated by certain synthetic chemical compounds that are exposed to a body via ingestion, inhalation, injection, dermal absorption, or other ways. Moreover, due to the very similar carcinogenesis process, chemically induced cancers mimic the human cancer occurrence from the initiation stage (6).

8.2 Methods

All experimental protocols for in vivo studies were reviewed and approved by Institutional Animal Ethics Committee, Pharmacy department, The M. S. University of Baroda, Vadodara, vide protocol approval no: MSU/IAEC/2021-22/2112. All the experimental procedures were carried out as per Committee for the Purpose of Control and Supervision of Experiments on Animals (CPCSEA) guidelines released by Department of Animal Husbandry and Dairying, Ministry of Fisheries Animal Husbandry and Dairying, Government of India (DAHD MoFAH&D).

8.2.1 Pharmacokinetic Study

Female Sprague Dawley (150-200g) were housed in cages placed in an animal room with a constant temperature of 25 °C and a fixed 12-hour light-dark cycle. The rats were given standard chow diet and water ad libitum. 42 rats were allocated in 7 groups randomly (Table 8.1). Animals were fasted 12 hours before starting the treatment. The samples were administered via intravenous tail vein injection and rats were further anaesthetized using isoflurane. Blood samples (not more than 1 ml) from retro-orbital plexus in heparinized microcentrifuge tubes at specified time intervals were collected. The rats were replenished with saline solution. Blood samples were centrifuged at 3500 rpm for 10 min at 4°C and harvested plasma was stored at -20°C until analysis using HPLC as described in Chapter 4, Section 4.10.3 (7).

Table 8.1: In vivo Pharmacokinetic study

Groups		Treatment
I.	Normal Control	0.9% saline
II.	Standard control I	Exemestane suspension (3.5mg/kg)
III.	Standard control II	Fulvestrant suspension (3.7 mg/kg)
IV.	Test group 1	FA-F-PLHNC (equivalent to 3.7 mg/kg fulvestrant)
V.	Test group 2	FQMSN (equivalent to 3.7 mg/kg fulvestrant and 5 mg/kg quercetin)
VI.	Test group 3	FA-E-PLHNC (equivalent to 3.5 mg/kg exemestane)
VII.	Test group 4	EQMSN (equivalent to 3.5 mg/kg exemestane and 5 mg/kg quercetin)

8.3 In vivo anticancer and biodistribution study

8.3.1 Tumor induction

Mammary tumors were induced using MNU (N-methyl, N-nitrosourea). MNU was dissolved immediately before use in 0.9% NaCl and adjusted with acetic acid to pH 4. The rats were given MNU intraperitoneally at a dose of 50 mg/kg body weight (5). The 6 rats of Normal control received sterile saline solution only. Rats were weighed weekly. After 3 weeks of MNU administration, they were palpated twice a week for presence of mammary tumor. When tumor was first palpated, its date and location were recorded.

8.3.2 Bio distribution study

The tumor bearing rats were divided into 12 groups of 3 animals each (Table 8.2). After 72 h of single dose administration, the animals were euthanized, and highly perfused organs such as spleen, liver, kidney, heart, and tumor were isolated and weighed (8). 30 % of tissue homogenate was prepared and stored at -30°C until further use. 200 µL of homogenate was diluted with 800 µL of ACN to precipitate the protein and the supernant was collected after centrifugation and analysed after suitable dilution by HPLC method as described in chapter 4, section 4.10.3 (9).

Table 8.3: Distribution of animal groups for In vivo anticancer studies

Groups		Treatment
I.	Drug Control I	FLV suspension (3.7 mg/kg)
II.	Drug Control II	EXE Suspension (3.5 mg/kg)
III.	Model Control	MNU (N-methyl, N-nitrosourea) in Sesame oil (50 mg/kg)
IV.	Test group 1	F-PLHNC (equivalent to 3.7 mg/kg fulvestrant)
V.	Test group 2	FA-F-PLHNC (equivalent to 3.7 mg/kg fulvestrant)
VI.	Test group 3	FMSN (equivalent to 3.7 mg/kg fulvestrant)
VII.	Test group 4	QMSN (5 mg/kg quercetin)
VIII.	Test group 5	FQMSN (equivalent to 3.7 mg/kg fulvestrant and 5 mg/kg quercetin)
IX.	Test group 6	E-PLHNC (equivalent to 3.5 mg/kg exemestane)
X.	Test group 7	FA-E-PLHNC (equivalent to 3.5 mg/kg exemestane)
XI.	Test group 8	EMSN (equivalent to 3.5 mg/kg exemestane)
XII.	Test group 9	EQMSN (equivalent to 3.5 mg/kg exemestane and 5 mg/kg quercetin)

8.3.3 In vivo anticancer study

When the tumor volume reached $\sim 1000 \text{ mm}^3$, animals were randomly divided into 15 different groups of 6 animals each (Table 8.3). The animals were treated with different formulations administered via intravenous route, once every week.

Table 8.3: Distribution of animal groups for In vivo anticancer studies

Groups		Treatment
I.	Normal Control	0.9% saline
II.	Model Control	MNU in 0.9% saline (50 mg/kg)
III.	Standard control I	Tamoxifen in sesame oil (1mg/kg)
IV.	Drug Control I	FLV suspension (3.7 mg/kg)
V.	Drug Control II	EXE Suspension (3.5 mg/kg)
VI.	Vehicle Control I	MNU(N-methyl, N-nitrosourea) in Sesame oil (50mg/kg)
VII.	Test group 1	F-PLHNC (equivalent to 3.7 mg/kg fulvestrant)
VIII.	Test group 2	FA-F-PLHNC (equivalent to 3.7 mg/kg fulvestrant)
IX.	Test group 3	FMSN (equivalent to 3.7 mg/kg fulvestrant)
X.	Test group 4	QMSN (5 mg/kg quercetin)
XI.	Test group 5	FQMSN (equivalent to 3.7 mg/kg fulvestrant and 5 mg/kg quercetin)
XII.	Test group 6	E-PLHNC (equivalent to 3.5 mg/kg exemestane)
XIII.	Test group 7	FA-E-PLHNC (equivalent to 3.5 mg/kg exemestane)
XIV.	Test group 8	EMSN (equivalent to 3.5 mg/kg exemestane)
XV.	Test group 9	EQMSN (equivalent to 3.5 mg/kg exemestane and 5 mg/kg quercetin)

8.4 Measurement of tumor growth and change in body weight

8.4.1 Body weight change:

Body weight of all the rats were recorded daily from the beginning of the experiment. The weight on the day when the animals were inoculated with MNU was denoted as day 0.

8.4.2 Tumor volume measurement:

Antitumor activity of different formulations was evaluated by measuring tumor growth inhibition. The tumor size was measured from the 10th day after MNU administration and the measurement was carried out every 5th day up to 6 weeks (10). The tumor volume was determined by the formula:

$$\text{Tumor volume} = L \cdot W^2 / 2 \quad (8.1)$$

Where, L is the length and W is the width of tumor mass.

8.4.3 Mean Survival percentage

The survival of tumor – bearing rats was observed until the tumor volume reached 50% above the ethical limit (1000 mm³) or death occurred after initiation of the treatments; whichever event was first observed was counted as death. From the survival data, mean survival percentage was calculated according to the following formula:

$$\text{Mean survival percentage} = \left(\frac{T}{C} - 1 \right) \times 100 \quad (8.2)$$

Where, T is mean survival time of treated rats and C is mean survival time of control rats

8.5 RESULTS AND DISCUSSION

8.5.1 In vivo pharmacokinetics of Fulvestrant loaded PLHNCs

An in vivo study was performed by estimating the fulvestrant concentration in blood after the administration of Fulvestrant suspension and FA PLHNCs (figure 8.2).

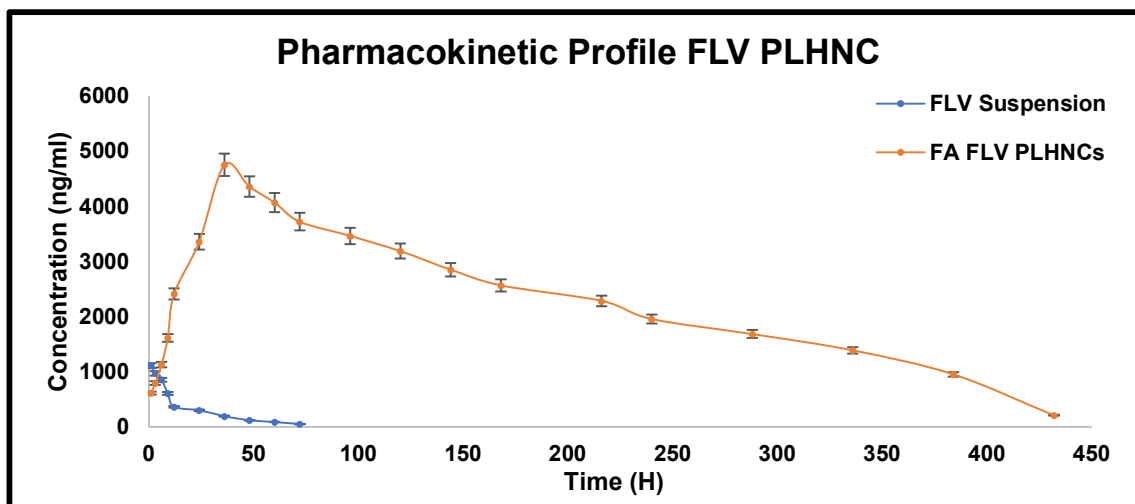


Figure 8.2 In vivo pharmacokinetic profile of fulvestrant

After intravenous administration, FLV suspension showed faster clearance with half-life of 16.94 ± 0.78 hrs. and AUC of 202.15 ± 9.68 ng/ml h. FA FLV PLHNCs showed the sustained release pattern with slower clearance rate with half-life of 12 days (16 times) and AUC of 4813.68 ± 189.62 ng/ml h (24 times). This sustained release can be due to presence of double barrier of polymer and lipid from which drug slowly diffused into blood. The slower clearance can be attributed to prolonged circulation of PLHNCs due to presence of PEGylation (9).

Table 8.4 Pharmacokinetic study of fulvestrant PLHNCs

Parameters	FLV Suspension	FA F-PLHNCs
$t_{1/2}$ (h)	16.94 ± 0.78	288.56 ± 12.59
AUC total, ng/ml, h	202.15 ± 9.68	4813.68 ± 189.62
C_{max} , ng/ml	1111.41 ± 4.87	4514.63 ± 136.98
T_{max}	2 ± 0.14	36 ± 1.4
V_d (ml)	4.02 ± 0.18	1.39 ± 0.057
C_0 (ng/ml)	92.37 ± 4.23	265.47 ± 12.14
Clearance (ml/h)	0.16 ± 0.007	0.003 ± 0.0001

8.5.2 In vivo pharmacokinetic study of Exemestane loaded PLHNCs

As seen in Figure. 8.3, after intravenous injection, EXE suspension showed rapid clearance with the half-life of 5.21 ± 0.22 hrs., and AUC of 933.23 ± 38.24 ng/ml h. Whereas, FA EXE PLHNCs, showed sustained release of the formulation with plasma half-life of 7 days (35 times) and AUC of 5221.07 ± 228.19 ng/ml h (5.6 times). The sustained release can be due to presence of double barrier of polymer and lipid from which drug slowly diffused into blood. The slower clearance can be attributed to prolonged circulation of PLHNCs due to presence of PEGylation

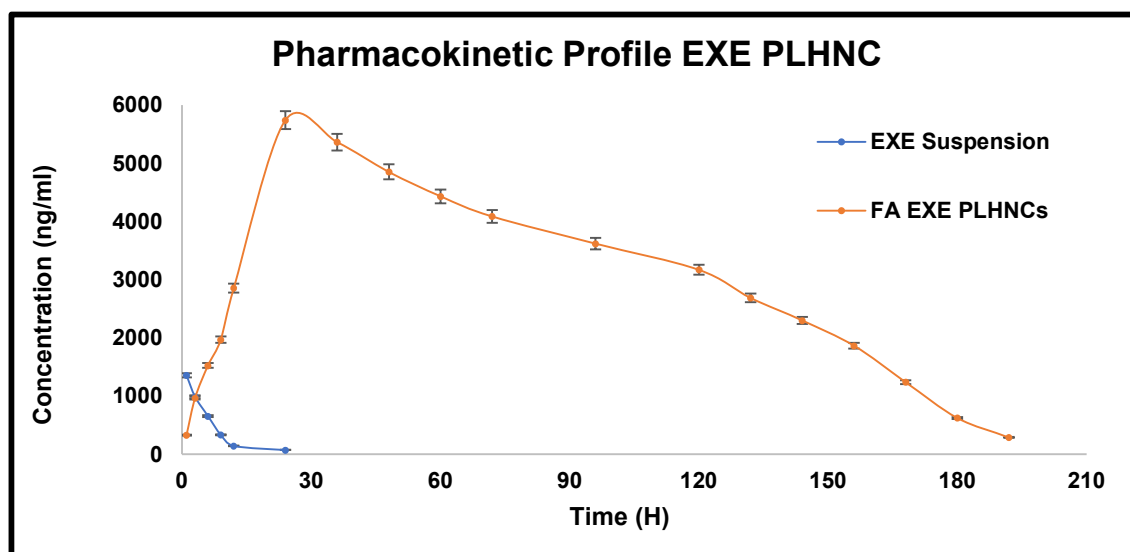


Figure 8.3 In vivo pharmacokinetic profile of exemestane

Table 8.5 Pharmacokinetic study of Exemestane PLHNCs

Parameters	EXE Suspension	FA EXE PLHNCs
$t_{1/2}$ (h)	5.21 ± 0.22	187.62 ± 7.25
AUC total, ng/ml, h	933.23 ± 38.24	5221.07 ± 228.19
C_{max} , ng/ml	1356.21 ± 4.18	5473.18 ± 214.79
T_{max} (hr)	2 ± 0.12	24.51 ± 1.68
V_d (ml)	2.89 ± 0.042	1.39 ± 0.051
C_0 (ng/ml)	127.92 ± 6.12	265.31 ± 12.84
Clearance (ml/h)	0.38 ± 0.0016	0.0051 ± 0.0003

8.5.3 In vivo pharmacokinetic study of Fulvestrant loaded MSNs

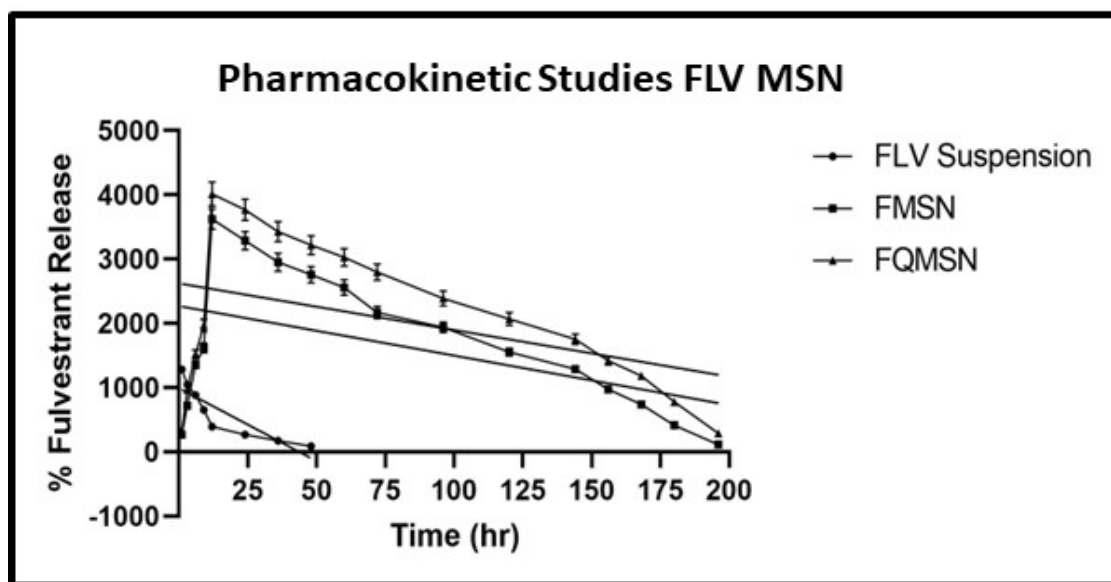


Figure 8.4 Pharmacokinetic data for fulvestrant formulations

The pharmacokinetic parameters of formulation administered via intravenous route were quite different from each other (figure 8.4). FLV suspension exhibited more rapid clearance from the blood with the $t_{1/2}$ of 12.61 hr and AUC of 187.67 ng/ml h. FLV loaded MSNs exhibited AUC of 2581.17 ng/ml h and a half-life of 105.98 h (8.40 times) as compared to FLV suspension (Table 8.5). FQMSN exhibited a slow and steady clearance with a longer half-life 167.24 h (13.26 times) and AUC 3764.41 ng/ml h as compared to free FLV and FMSN. The pharmacokinetics data were significant ($p < 0.0044$, $R^2 = 0.9162$).

Table 8.6 Pharmacokinetic study of fulvestrant MSNs

Parameters	FLV Suspension	FMSN	FQMSN
$t_{1/2}$ (h)	12.61 ± 0.54	105.98 ± 4.23	167.24 ± 6.41
AUC total, ng/ml, h	187.67 ± 8.68	2581.37 ± 110.65	3764.41 ± 136.84
C _{max} , ng/ml	1045.84 ± 36.54	3621.35 ± 134.29	4012.36 ± 225.21
T _{max} (hr)	3.62 ± 0.14	16.51 ± 1.04	17.18 ± 1.36
V _d (ml)	3.30 ± 0.15	1.82 ± 0.008	1.64 ± 0.007
C ₀ (ng/ml)	111.87 ± 4.98	203.39 ± 8.56	224.34 ± 9.68
Clearance (ml/h)	0.181 ± 0.007	0.011 ± 0.0005	0.0067 ± 0.0004

8.5.4 In vivo pharmacokinetic study of Exemestane loaded MSNs

The pharmacokinetic parameters of formulations administered via intravenous route were quite different. EXE suspension exhibited a more rapid clearance from blood with the half-life of 5.92 h and AUC of 1206.9 ng/ml h. EMSN exhibited a half-life of 85.83 h and AUC of 2945.67 ng/ml h which was 14.49 times and 2.44 times more respectively. EQMSN exhibited a slow and steady clearance with much longer half-life of 120.69 h and higher AUC of 3852.85 ng/ml h, which was 20.38 times and 3.19 times respectively more compared to EXE suspension and 1.40 times and 1.30 more than that of EMSN. The pharmacokinetics data were significant ($p < 0.0084$, $R^2 = 0.8912$).

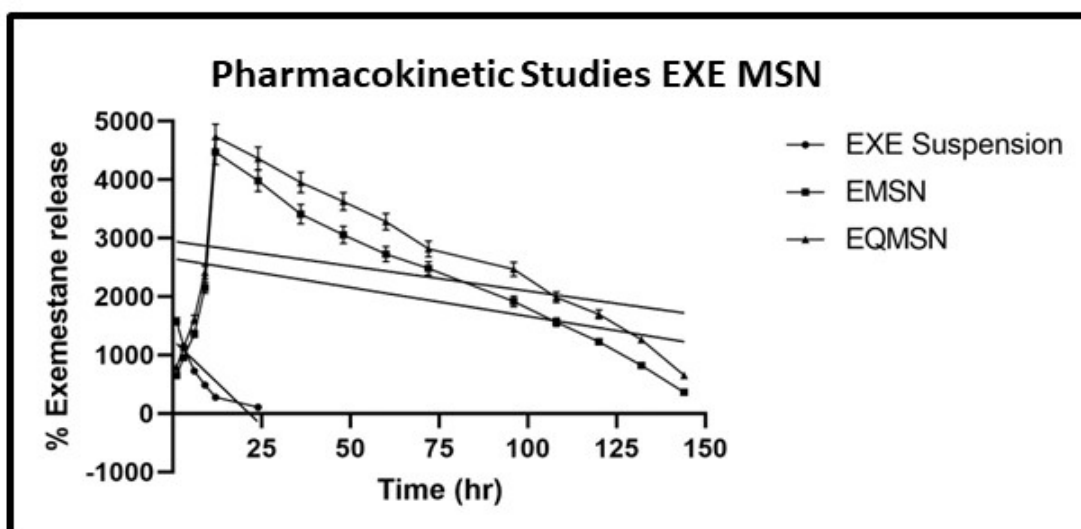


Figure 8.5 Pharmacokinetic data for exemestane MSN formulations

Table 8.7 Pharmacokinetic study of exemestane formulations

Parameters	EXE Suspension	EMSN	EQMSN
$t_{1/2}$ (h)	5.92 ± 0.24	85.83 ± 3.87	120.69 ± 5.41
AUC total, ng/ml, h	1206.9 ± 5.21	2945.67 ± 132.52	3852.85 ± 168.17
C_{max} , ng/ml	1578.87 ± 4.84	4473.18 ± 151.26	4739.12 ± 19.85
T_{max} (hr)	3.12 ± 0.14	16.84 ± 1.36	17.41 ± 1.68
V_d (ml)	2.44 ± 0.09	1.56 ± 0.072	1.43 ± 0.067
C_0 (ng/ml)	151.61 ± 7.12	235.89 ± 10.36	257.34 ± 12.25
Clearance (ml/h)	0.29 ± 0.014	0.009 ± 0.0005	0.005 ± 0.0003

8.5.5 Biodistribution studies

8.5.5.1 Biodistribution studies of Fulvestrant loaded PLHNCs

The bio-distribution studies of the formulation were carried out and concentration of FLV in different organs was determined. It could be inferred that the concentration of FLV from FLV PLHNCs and FA FLV PLHNCs was remarkably high in tumor cells compared to other major organs and compared with FLV suspension (Figure 8.6). This might be due to prolonged circulation of the formulation and FA conjugation that targets the drug towards tumor cells and increases its uptake by breast cancer cells. This will improve the therapeutic efficacy and reduce its systemic side effects.

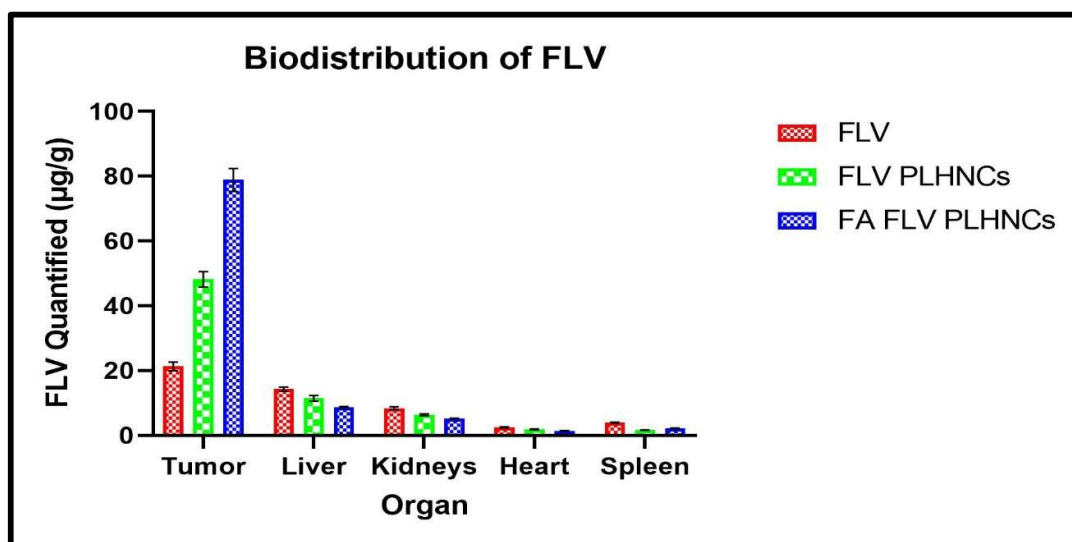


Figure 8.6 Biodistribution of FLV PLHNCs formulations

The lipid based formulations are prone to be cleared by the liver and spleen by RES clearance, though here PLHNCs prepared were having PEG coat that prevents the uptake of liposomes by liver and spleen. FLV concentration in liver with suspension was found to be higher and it is reported to increase AST levels, indicating liver injury. Here with FLV PLHNCs and FA FLV PLHNCs the FLV distribution was found to reduce to 30% and 50% respectively, indicating reduction in chances of liver injury. FLV concentration, however, plays a significant role in cardiovascular muscles, as according to Omer et. al it was reported to increase arrhythmias in ischemic patients which may be dependent on the increased repolarization and shortening of the action potential in the myocardial cells caused by the blockage of the inward calcium current through the L-type calcium channel and on the opening of the outward potassium current through the BK channel (11).

8.5.5.2 Biodistribution studies of Exemestane loaded PLHNCs

The biodistribution studies carried out for EXE PLHNCs formulations supported the theoretical aspect of increased uptake of folic acid conjugated nanoparticles (Figure 8.7). The results showed higher concentration of EXE within tumor cells compared to other organs (12). The concentration of EXE with FA EXE PLHNCs was found to be higher in tumor cells compared to EXE PLHNCs and EXE suspension, suggesting preferential accumulation of nanoparticles in tumor cells due to receptor mediated endocytosis. However, higher biodistribution of EXE PLHNCs was found in liver due opsonization of the nanoparticles and clearance by tissue macrophages of the RES (13).

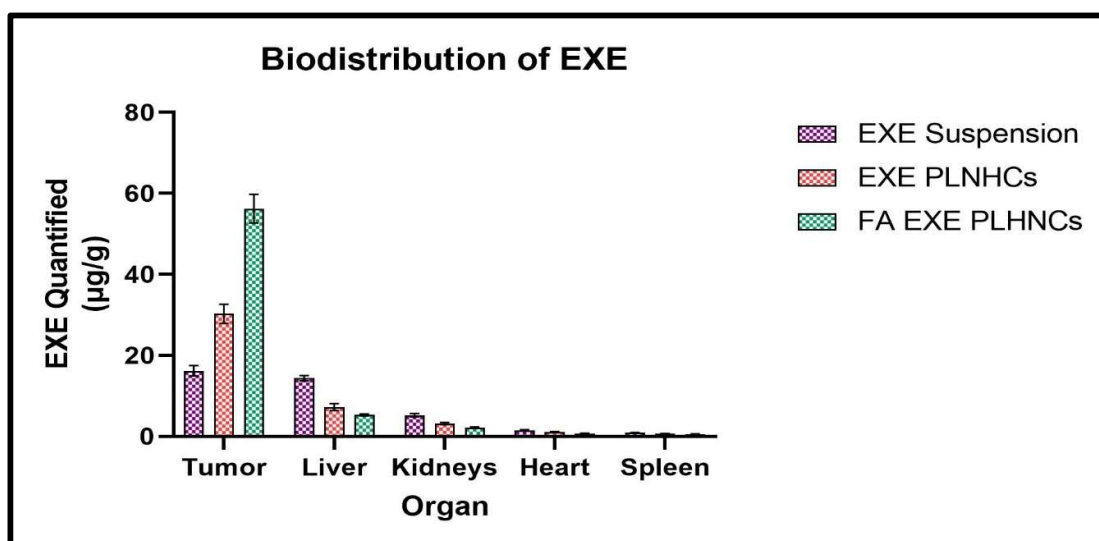


Figure 8.7 Biodistribution of EXE PLHNCs formulations

8.5.5.3 Biodistribution studies of fulvestrant loaded MSNs

The biodistribution studies carried out for Fulvestrant MSN formulations and FLV suspension, showed the increased cellular uptake of FLV with FMSN and FQMSN by the tumor cells and reduced the overall distribution of drug in other organs (Figure 8.8). The increased uptake and efficacy of Fulvestrant with quercetin can be attributed to the prevention of metabolism and resistance by quercetin via prevention of PI3KCA mutation which is stated to be the primary cause for FLV resistance in breast cancer cells (14).

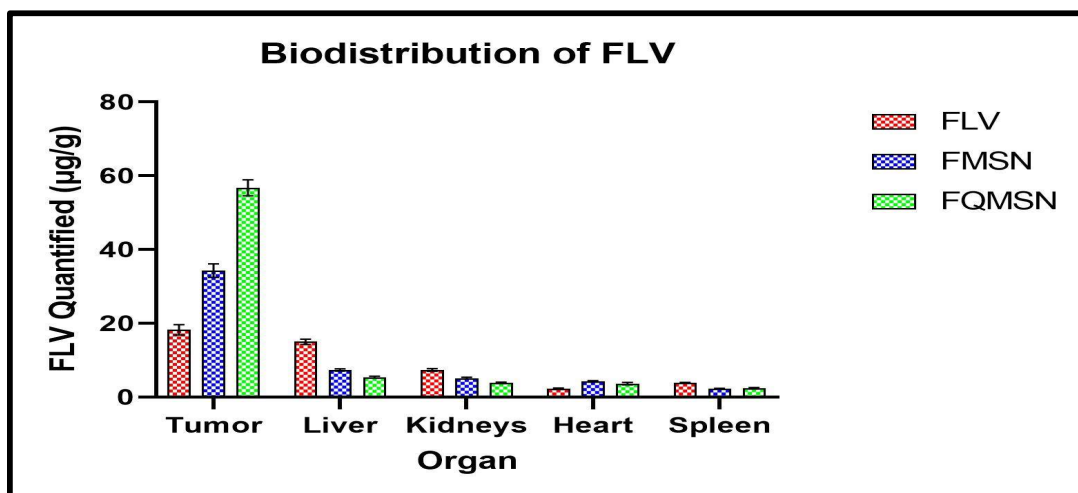


Figure 8.8 Biodistribution of FLV MSN formulations

8.5.5.4 Biodistribution studies of Exemestane loaded MSNs

The biodistribution studies carried out for Exemestane MSN formulations and EXE suspension, showed the increased cellular uptake of EXE with EMSN and EQMSN by the tumor cells and reduced the overall distribution of drug in other organs, specifically liver which brings about rapid metabolism of EXE in case of EXE suspension. The increased uptake and efficacy of Exemestane with quercetin can be attributed to the reduction in metabolism and tumor resistance

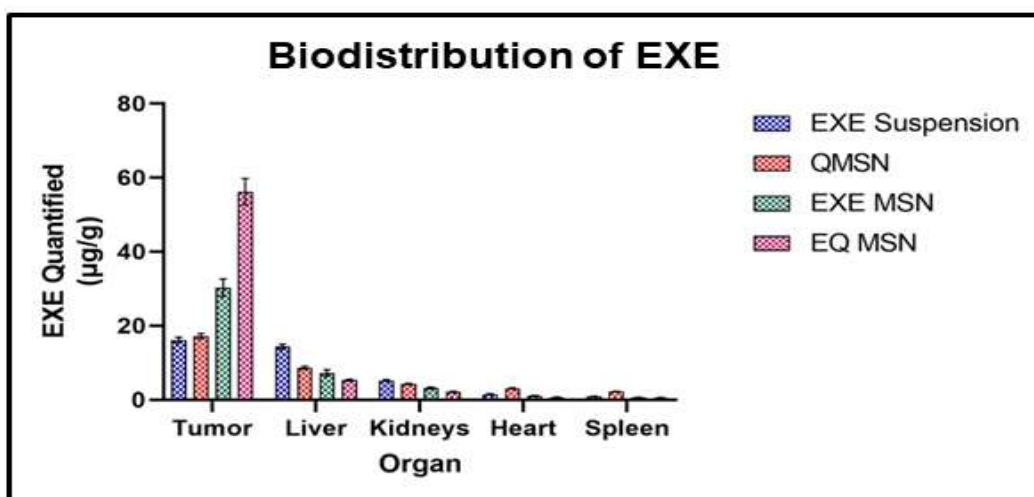


Figure 8.9 Biodistribution of EXE MSN formulations

8.5.6 Body weight change

Figures 8.10 and 8.11 represent average change in the body weight of the animals as a function of time after initiation of tumour growth. The model control group, injected with MNU and receiving no treatment showed significant weight gain while the groups receiving tamoxifen suspension, fulvestrant suspension and exemestane suspension showed significant weight loss.

An initial increase in the weight of all rats (except normal control) was observed after tumor inoculation. Model control group continuously showed increase in the weight till the animal death. This increase in the weight was due to the presence of ascitic fluid (observed when the sacrificed rats were dissected). The group receiving drug suspension alone showed significant weight reduction and it was considerably different from the weight of model control group ($p < 0.0001$). Apart from that, there was slight reduction in hairs of the rats receiving FLV and exemestane suspension alone owing to the side effects of chemotherapeutic agent. Animals treated with NPs showed significant difference in weight ($p < 0.001$) when compared with model control group and also there was significant weight reduction due to reduction in tumor burden (15). There was a significant reduction in the weight of animals treated with FLV suspension and standard group as they present serious systemic side effects such as loss of appetite and muscle loss. Studies suggest if Tamoxifen is taken for more than a week, it promotes weight loss due to activation of cytokines that promote muscle loss (16).

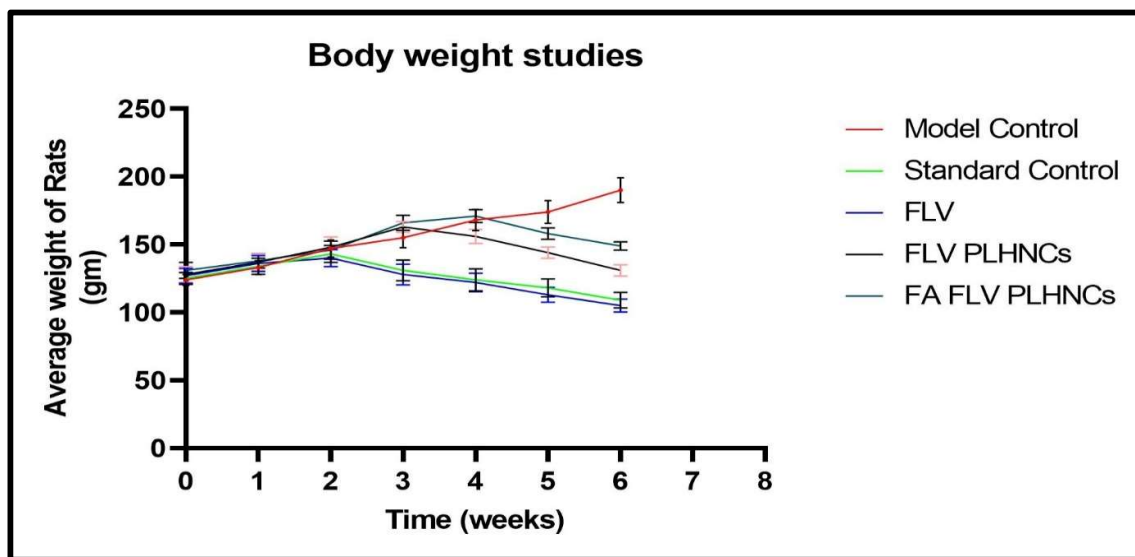


Figure 8.10 (A) Body weight studies for fulvestrant PLHNCs formulations

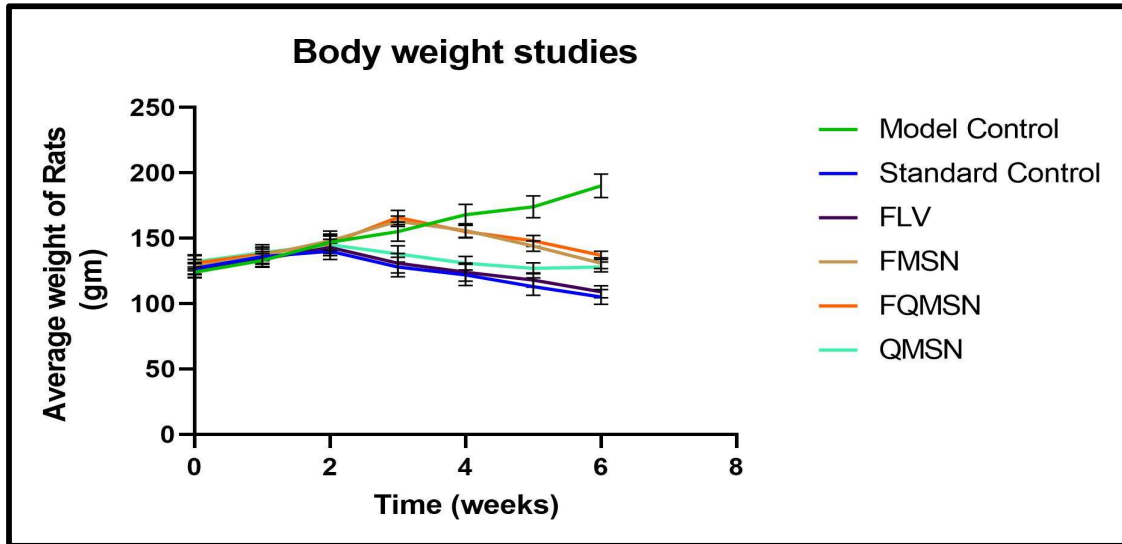


Figure 8.10 (B) Body weight studies for FLV MSNs formulations

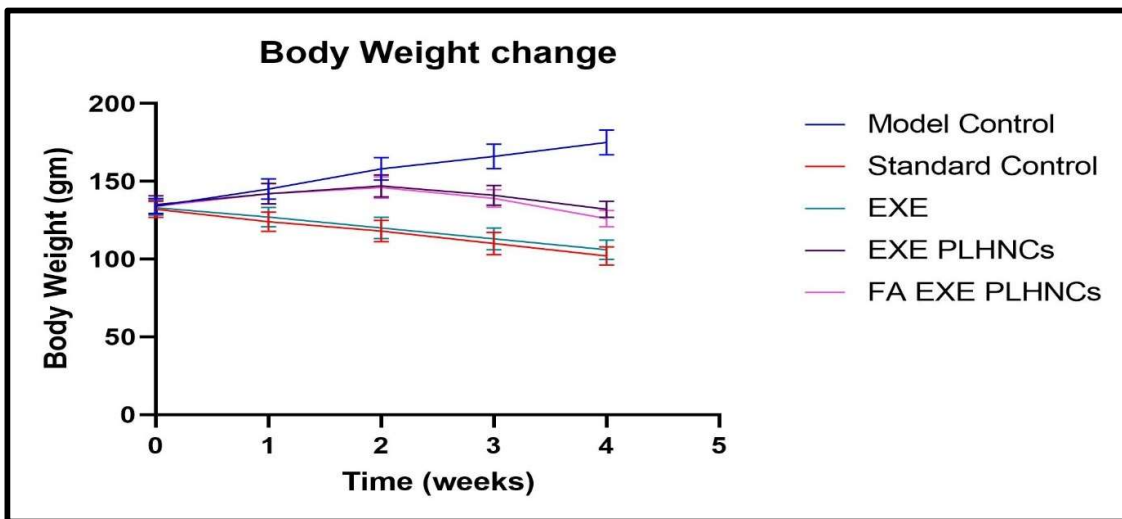


Figure 8.11 (A) Body weight studies for EXE PLHNCs formulations

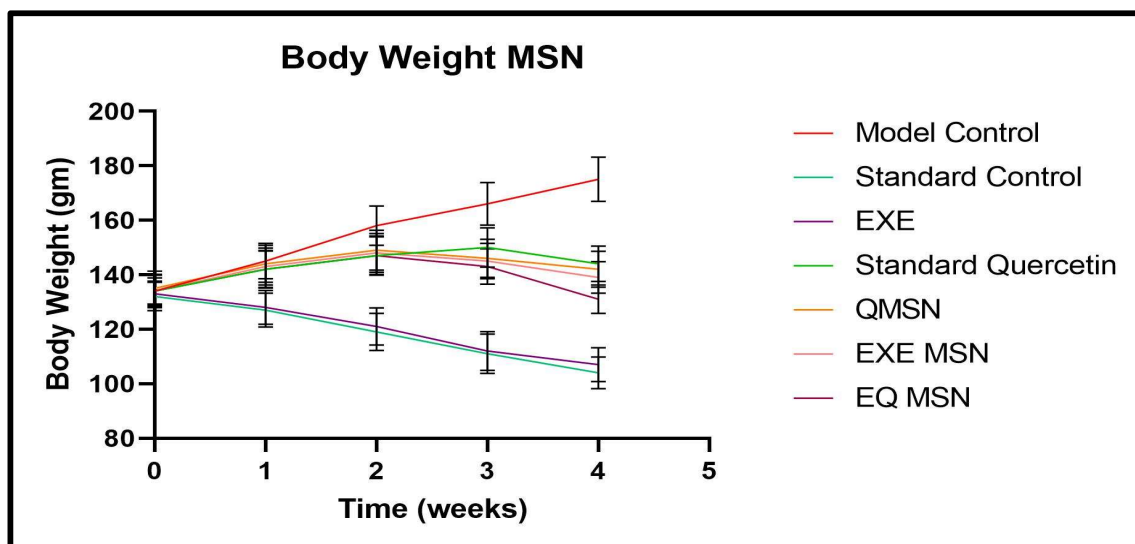


Figure 8.11 (B) Body weight studies for EXE MSNs formulations

8.5.7 Tumor regression study for fulvestrant formulations

Figure 8.12 (A & B) corresponds to change in tumor volume as a function of time. In figure 8.12, it was clearly seen that the tumor continued to grow in model control group while it was significantly suppressed in treatment groups ($p < 0.001$ when compared to with the model control group). A significant difference in the tumor volume was measured after completion of treatment (6 weeks for PLHNCs and 4 weeks for MSNs). FA FLV PLHNCs and FQMSN showed maximum and better tumor inhibition ($p < 0.0001$). FLV PLHNCs and FMSN restricted the tumor growth and reduction in tumor volume, though complete shrinkage was not observed. The superior anticancer of FA FLV PLHNCs and FQMSN was attributed to increased cellular uptake and folic acid conjugation on its surface that targets the drug to folate receptors overexpressed in breast cancer cells (17). Quercetin played a significant role in reduction of tumor volume as it prevents the resistance of tumor cells offered against the fulvestrant treatment by inhibition of PI3KCA enzyme which is one of the mechanisms of quercetin treatment. Quercetin is also proven to promote cellular apoptosis by increase in ROS in tumor cells (14).

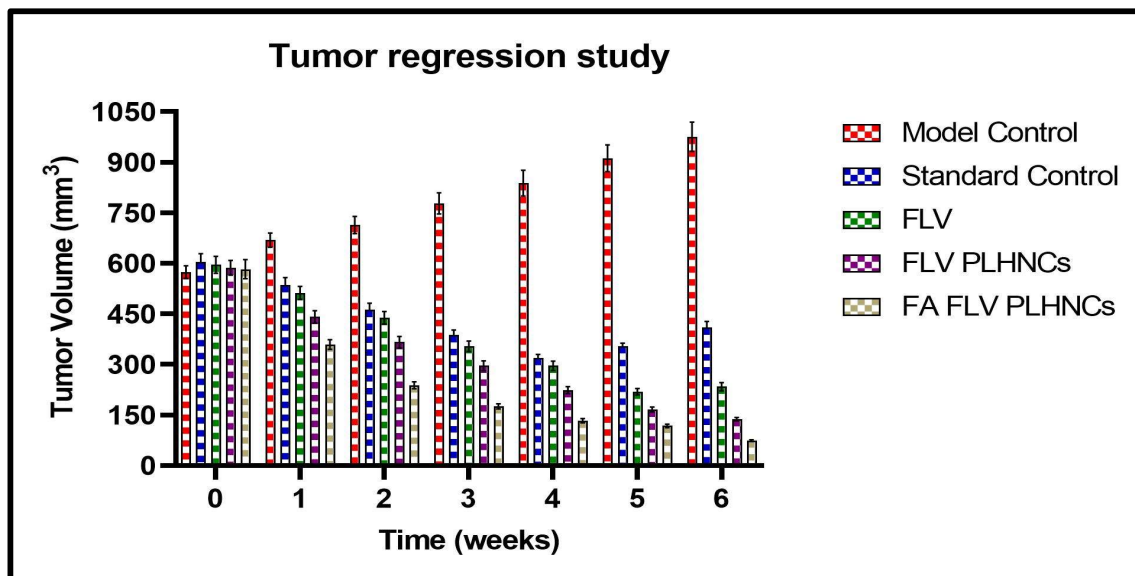


Figure 8.12 (A) Tumor regression study for FLV PLHNCs formulations

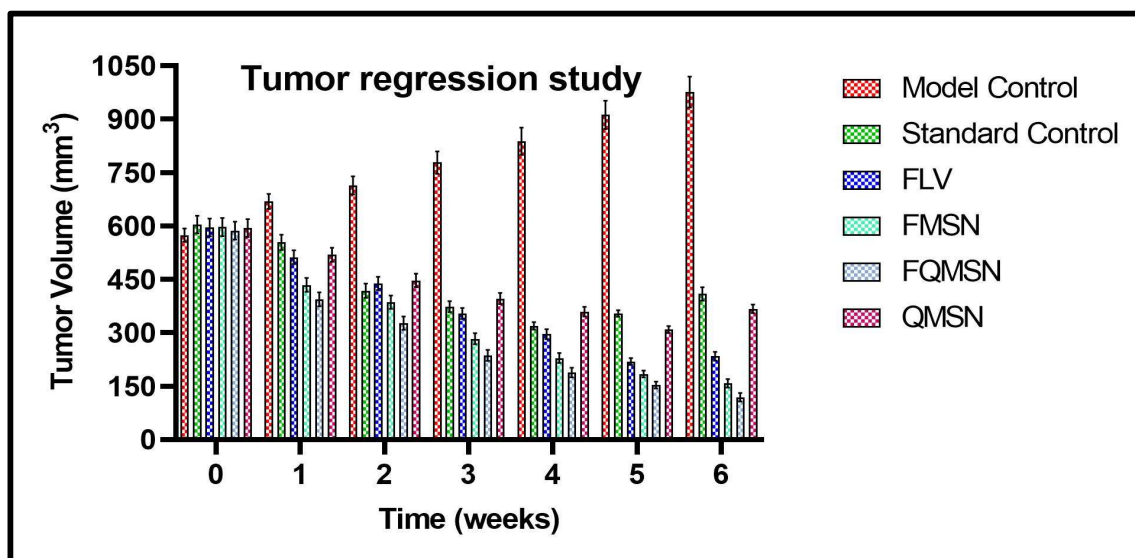


Figure 8.12 (B) Tumor regression study for FLV MSNs formulations

8.5.8 Tumor volume (Exemestane)

In figure 8.13, it is clearly seen that the tumor continued to grow in model control group while it was significantly suppressed in treatment groups ($p < 0.0001$) when compared to with the model control group). A significant difference in the tumor volume was measured after completion of treatment (4 weeks). FA EXE PLHNCs and EQMSN showed maximum and better tumor inhibition ($p < 0.001$). EXE PLHNCs and EMSN restricted the tumor growth and reduced the tumor volume compared to exemestane suspension.

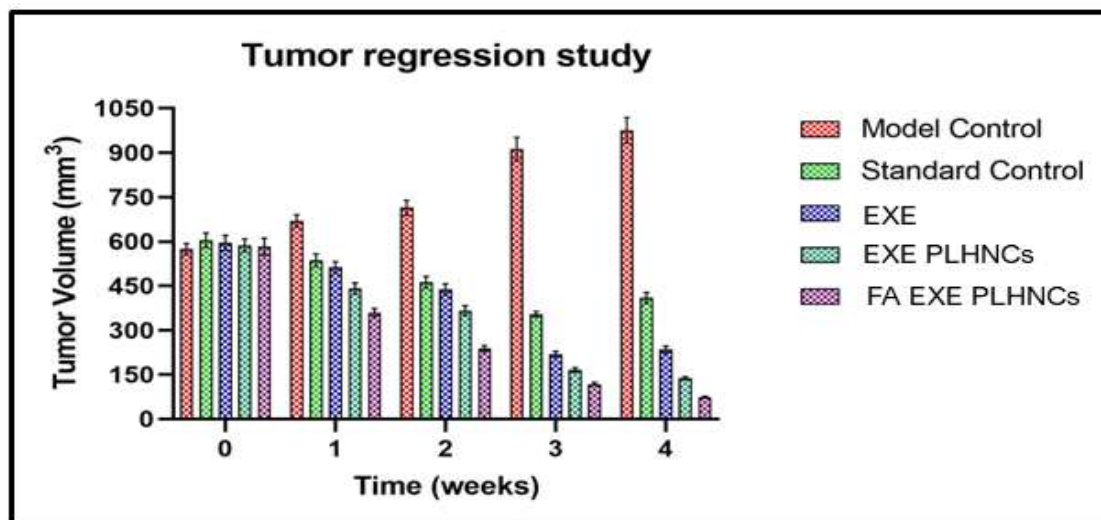


Figure 8.13 (A) Tumor regression study for EXE PLHNCs formulations

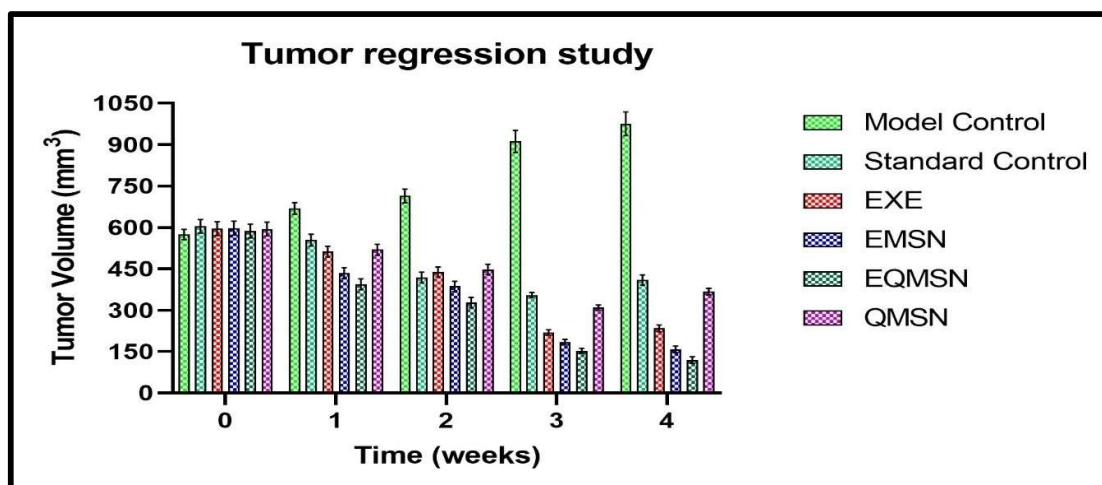


Figure 8.13 (B) Tumor regression study for EXE MSNs formulations

8.5.9 Survival curve (Kaplan Meier plot) (Fulvestrant)

The survival rate for different experimental rats inoculated with MNU were monitored up to 12 weeks after first tumor palpitation. The Kaplan Meier survival plot was plotted for better understanding (figure 8.14a). The rats treated with standard control showed 50 % survival, those treated with fulvestrant suspension showed 66.67% survival, those treated with FLV PLHNCs showed 83.33% survival whereas the animals treated with FA FLV PLHNCs showed 100% survival during treatment (6 weeks).

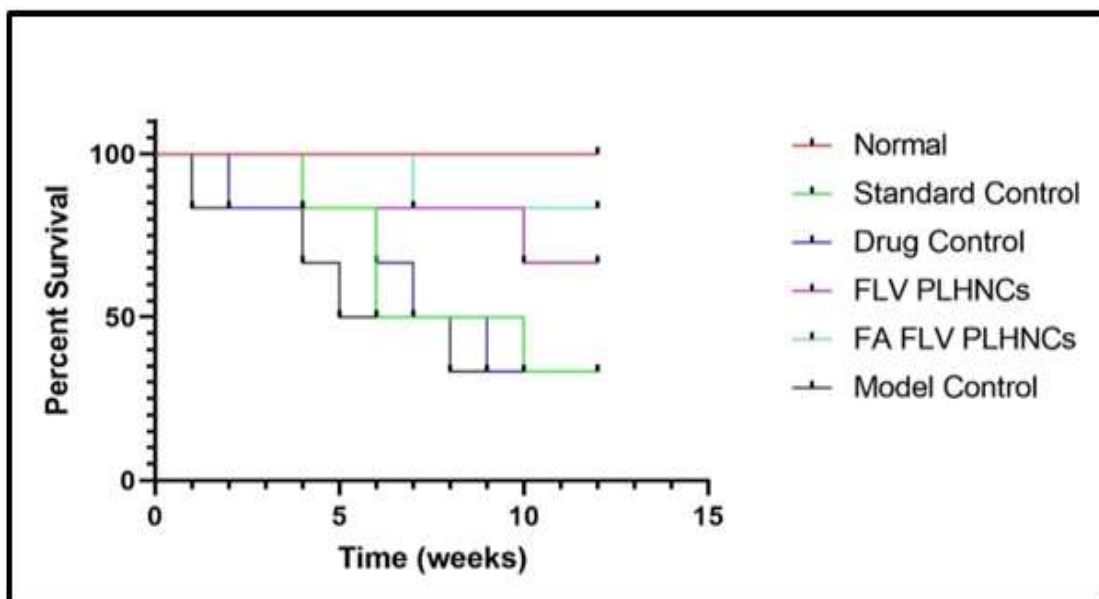


Figure 8.14 (a) Kaplan Meier Survival curve for FLV PLHNCs formulations

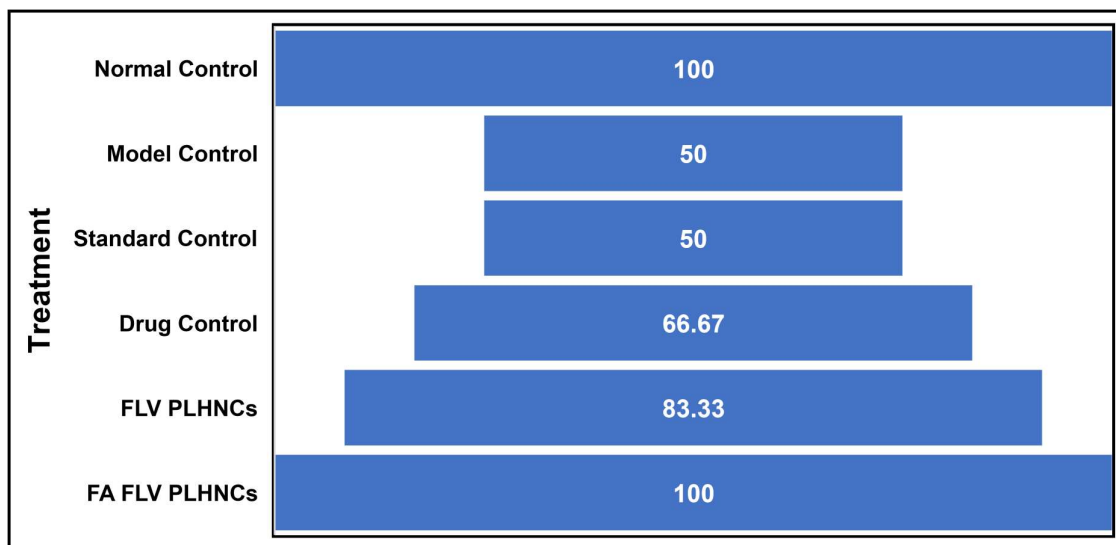


Figure 8.14 (b) Mean Survival Percentage for FLV PLHNCs formulations

The data of survival study postulated that the nanoparticles prolonged the survival of the animals, as the samples treated with standard and drug control showed death of 50 % animals (3 animals) within the course of treatment (6 weeks), whereas with FMSN, there was death of only 13.33 % of animals (1 animal). The animals treated with FQMSN showed no death and had 100 % survival up to 6 weeks. So, it can be said that FQMSN showed 100 % survival rate during treatment as opposed to standard and drug control that had only 50 % survival rate.

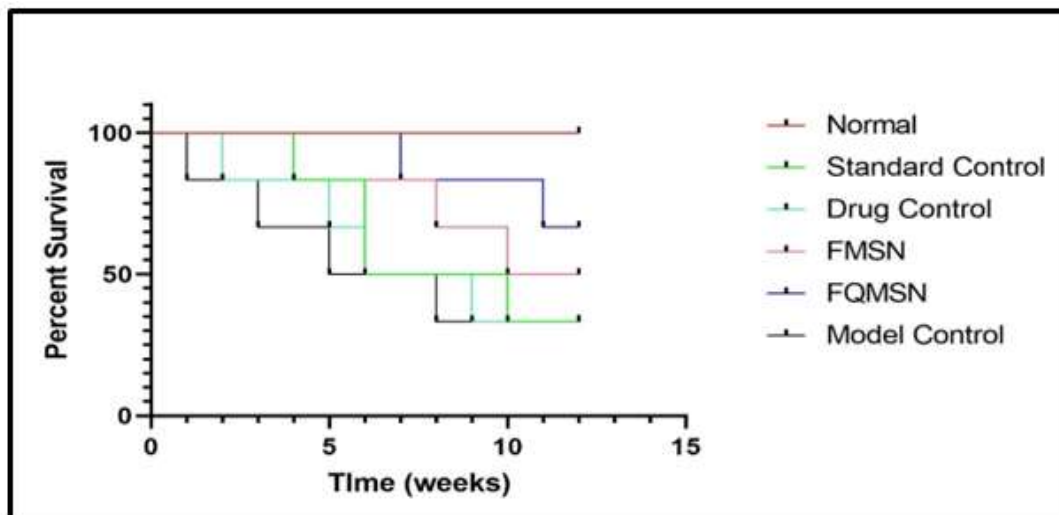


Figure 8.15 (a) Kaplan Meier Survival curve for FLV MSNs formulations

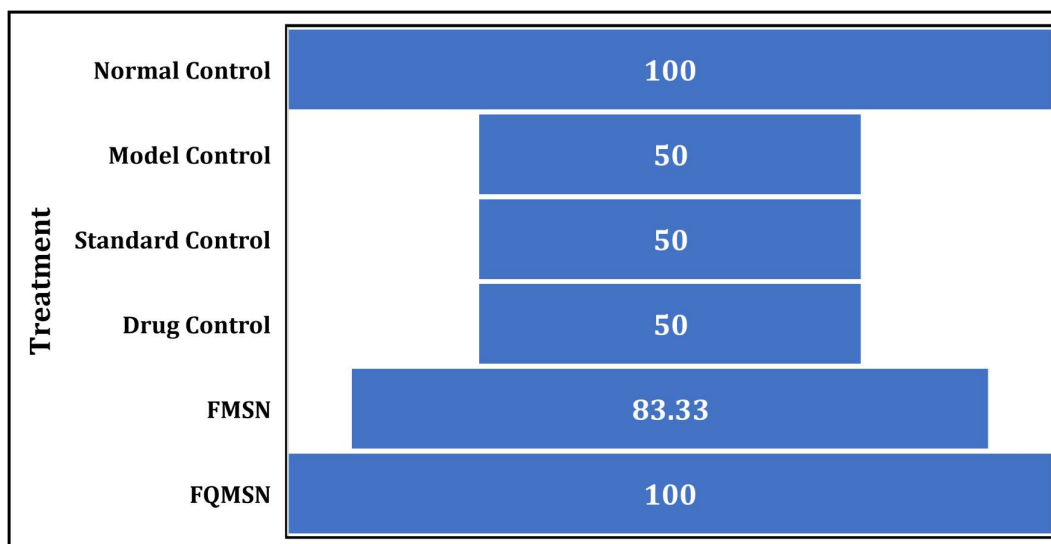


Figure 8.15 (b) Mean Survival Percentage for FLV MSN formulations

8.5.10 Survival curve (Kaplan Meier plot) (Exemestane)

The rats treated with standard and drug control showed 50% and 66.67% survival respectively, whereas rats treated with EXE PLHNCs showed 83.33% survival and FA EXE PLHNCs showed 100 % up to the course of treatment which suggested the improvement of efficacy of EXE with NPs compared to EXE suspension.

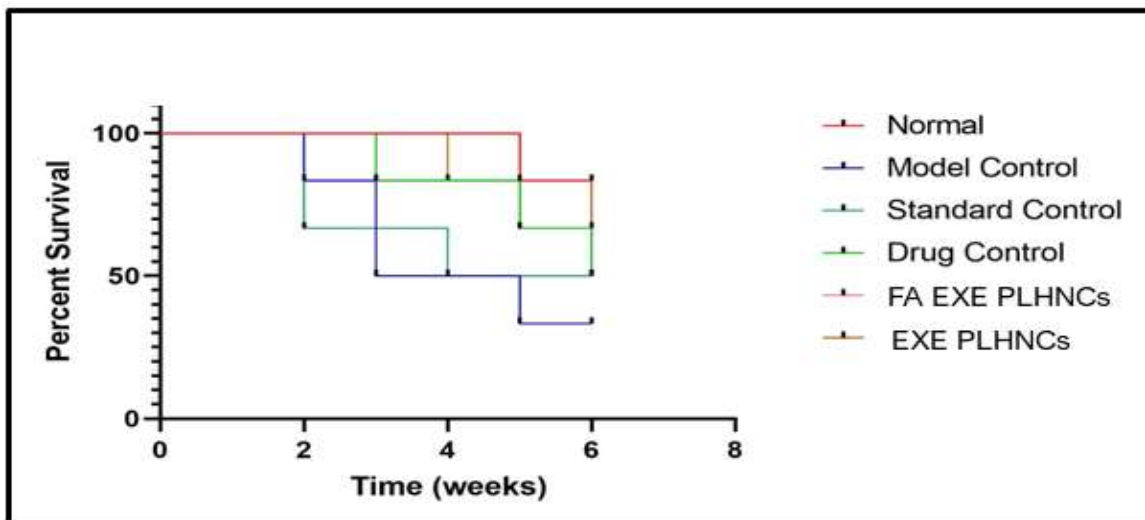


Figure 8.16 (a) Kaplan Meier Survival curve for EXE PLHNCs formulations

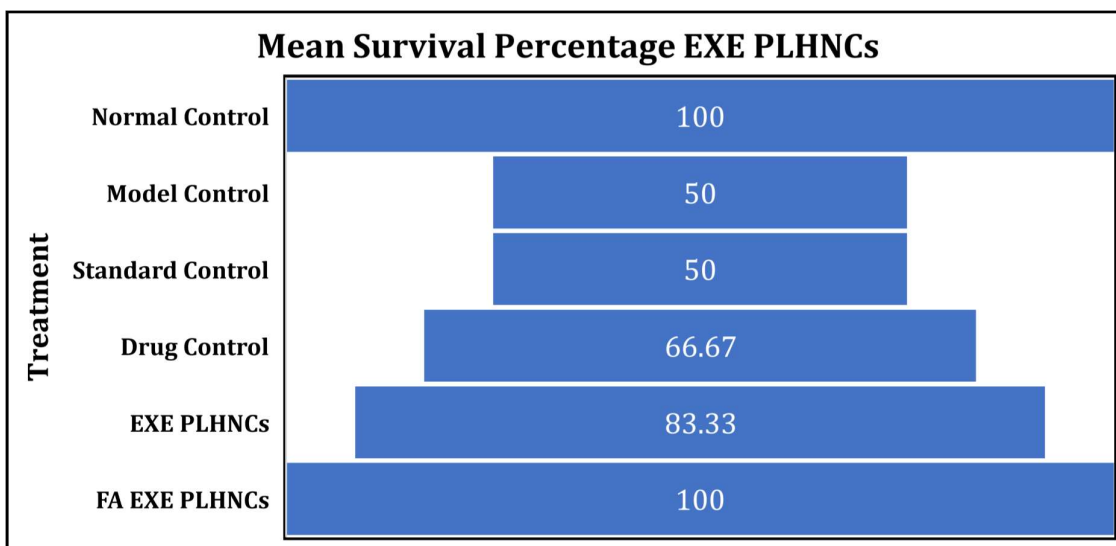


Figure 8.16 (b) Mean Survival Percentage for EXE PLHNCs formulations

The rats treated with standard and drug control showed 50% survival. The samples treated with QMSN showed 66.67% survival which is 1.33 times more compared to its standard counterpart and standard drug sample. The sample with EMSN showed 83.33% survival which is 1.66 times more compared to standard and drug control. EQMSN showed 100% survival which was 1.20 times more than that of EMSN, whereas 2 times more than that of the standard and model control.

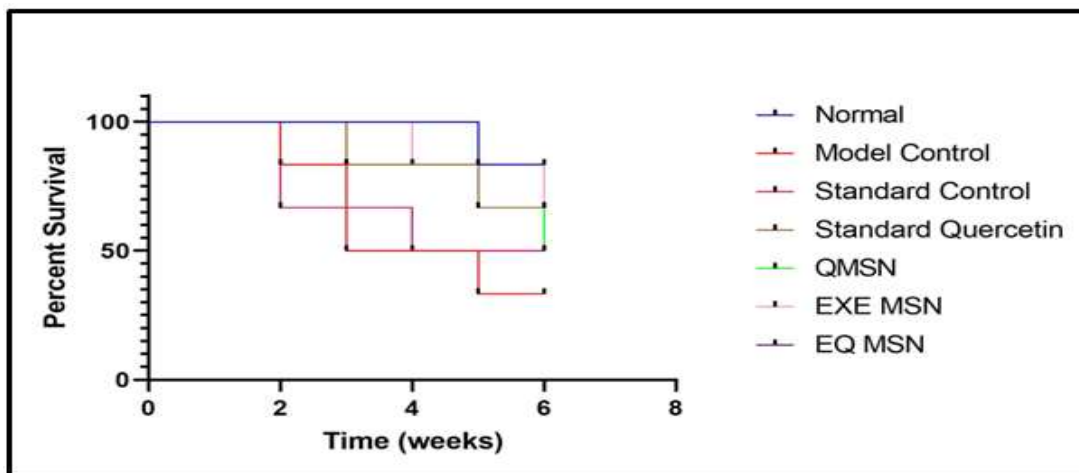


Figure 8.17 (a) Kaplan Meier Survival curve for EXE MSNs formulations

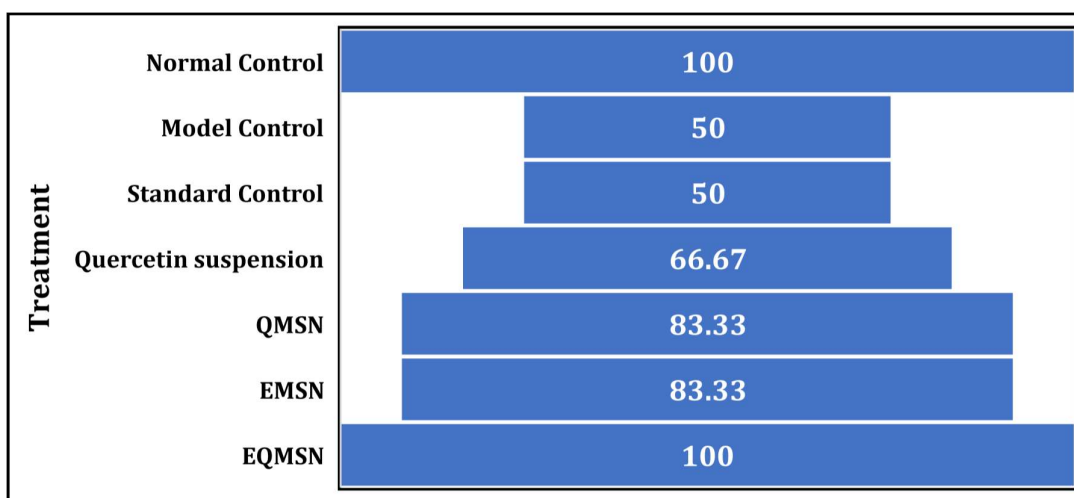


Figure 8.17 (b) Mean Survival Percentage for EXE MSNs formulations

8.6 Conclusion

The results suggested that the developed folate conjugated PLHNCs and folate conjugated quercetin co loaded mesoporous silica nanoparticles with fulvestrant and exemestane have potential to target the breast cancer cells and reduce their toxicity towards normal cells. The pharmacokinetic studies also supported the prolonged drug release from the NPs. The biodistribution studies showed increased concentration of drugs from folate conjugated NPs within tumor cells. The in vivo anticancer activity carried out on MNU induced rat tumor model showed reduction in overall tumor burden and increased survival rate of animals.

References

1. Yalcin TE, Ilbasmis-Tamer S, Takka S. Antitumor activity of gemcitabine hydrochloride loaded lipid polymer hybrid nanoparticles (LPHNs): In vitro and in vivo. *International journal of pharmaceutics*. 2020;580:119246.
2. Gray MA, Stanczak MA, Mantuano NR, Xiao H, Pijnenborg JFA, Malaker SA, et al. Targeted glycan degradation potentiates the anticancer immune response in vivo. *Nature chemical biology*. 2020;16(12):1376-84.
3. Mohr CJ, Schroth W, Mürdter TE, Gross D, Maier S, Stegen B, et al. Subunits of BK channels promote breast cancer development and modulate responses to endocrine treatment in preclinical models. *British Journal of Pharmacology*. 2022;179(12):2906-24.
4. Landgraf M, McGovern JA, Friedl P, Hutmacher DW. Rational design of mouse models for cancer research. *Trends in biotechnology*. 2018;36(3):242-51.
5. Alvarado A, Lopes AC, Faustino-Rocha AI, Cabrita AMS, Ferreira R, Oliveira PA, et al. Prognostic factors in MNU and DMBA-induced mammary tumors in female rats. *Pathology-Research and Practice*. 2017;213(5):441-6.
6. Faustino-Rocha AI, Gama A, Oliveira PA, Alvarado A, Neuparth MJ, Ferreira R, et al. Effects of lifelong exercise training on mammary tumorigenesis induced by MNU in female Sprague–Dawley rats. *Clinical and experimental medicine*. 2017;17(2):151-60.
7. Poonia N, Kaur Narang J, Lather V, Beg S, Sharma T, Singh B, et al. Resveratrol loaded functionalized nanostructured lipid carriers for breast cancer targeting: Systematic development, characterization and pharmacokinetic evaluation. *Colloids and Surfaces B: Biointerfaces*. 2019;181:756-66.
8. Ernsting MJ, Murakami M, Roy A, Li S-D. Factors controlling the pharmacokinetics, biodistribution and intratumoral penetration of nanoparticles. *Journal of Controlled Release*. 2013;172(3):782-94.
9. He Z, Huang J, Xu Y, Zhang X, Teng Y, Huang C, et al. Co-delivery of cisplatin and paclitaxel by folic acid conjugated amphiphilic PEG-PLGA copolymer nanoparticles for the treatment of non-small lung cancer. *Oncotarget*. 2015;6(39):42150.
10. Pritt B, Ashikaga T, Oppenheimer RG, Weaver DL. Influence of breast cancer histology on the relationship between ultrasound and pathology tumor size measurements. *Modern pathology*. 2004;17(8):905-10.
11. Bozdogan O, Bozcaarmutlu A, Kaya ST, Sapmaz C, Ozarslan TO, Eksioglu D, et al. Decreasing myocardial estrogen receptors and antioxidant activity may be responsible for increasing ischemia- and reperfusion-induced ventricular arrhythmia in older female rats. *Life Sciences*. 2021;271:119190.
12. Muhamad N, Plengsuriyakarn T, Na-Bangchang K. Application of active targeting nanoparticle delivery system for chemotherapeutic drugs and traditional/herbal medicines in cancer therapy: a systematic review. *International journal of nanomedicine*. 2018;13:3921.
13. Yoo M-K, Park I-K, Lim H-T, Lee S-J, Jiang H-L, Kim Y-K, et al. Folate–PEG–superparamagnetic iron oxide nanoparticles for lung cancer imaging. *Acta Biomaterialia*. 2012;8(8):3005-13.
14. Liu J, Li J, Wang H, Wang Y, He Q, Xia X, et al. Clinical and genetic risk factors for Fulvestrant treatment in post-menopause ER-positive advanced breast cancer patients. *Journal of Translational Medicine*. 2019;17(1):27.
15. Krell J, Januszewski A, Yan K, Palmieri C. Role of fulvestrant in the management of postmenopausal breast cancer. *Expert Review of Anticancer Therapy*. 2011;11(11):1641-52.
16. Ibrahim OM, El-Deeb NM, Abbas H, Elmasry SM, El-Aassar MR. Alginate based tamoxifen/metal dual core-folate decorated shell: Nanocomposite targeted therapy for breast cancer via ROS-driven NF- κ B pathway modulation. *International journal of biological macromolecules*. 2020;146:119-31.
17. Massarweh S, Osborne CK, Jiang S, Wakeling AE, Rimawi M, Mohsin SK, et al. Mechanisms of tumor regression and resistance to estrogen deprivation and fulvestrant in a model of estrogen receptor–positive, HER-2/neu-positive breast cancer. *Cancer research*. 2006;66(16):8266-73.